

# Graph Classification using Signal Subgraphs

Joshua T. Vogelstein, William R. Gray, R. Jacob Vogelstein, and Carey E. Priebe

**Abstract**—While there has been much recent interest in statistical inference, most work operates on vector-valued objects. In this manuscript, we consider the following “graph classification” question: given a collection of graphs and associated classes, how can we predict the class of a newly observed graph? To address this question we propose a statistical model for graph/class pairs. Given this model, we devise a set of estimators to find the class-conditional signal, referred to here as the “signal subgraph.” The classifiers differ by their assumption about the “coherency” of the signal subgraph, that is, what is the minimum number of vertices to which all signal subgraph edges are incident. Which estimator works best is shown to be a function not just of the coherency of the model, but also of the number of training samples. These estimators are employed on an interesting neuroscience question: can we classify connectomes according to gender. The answer is yes, significantly better than a naïve strategy. Synthetic data analysis demonstrates that even if the model were correct, given the relatively small number of data samples, the estimated signal subgraph should be taken with a grain of salt. We conclude by discussing several possible extensions.

**Index Terms**—statistical inference, graph theory, network theory, structural pattern recognition, connectome.



## 1 INTRODUCTION

GRAPHS are becoming increasingly popular vehicles for data representation, spanning fields from optical character recognition and chemistry [1], to neuroscience [2]. While statistical inference techniques for vector-valued data are widespread, statistical tools for the analysis of graph-valued data are relatively rare [1]. In this work we consider the task of *graph classification*: given a collection of graphs and their corresponding classes, can we accurately estimate the class of a new graph lacking a class label? We propose and analyze a joint graph/class model—sufficiently simple to characterize its asymptotic properties, and sufficiently rich to afford useful empirical applications. This model admits a class-conditional signal encoded in a subset of edges, the *signal subgraph*. Finding the signal subgraph amounts to providing an understanding of what are the differences between the two classes of graphs. Moreover, we are interested in learning to what extent this signal is “coherent”, that is, to what extent are all the edges incident to a relatively small set of vertices. This approach is qualitatively different from most previous approaches which utilize only (i) vertex labels or (ii) graph structure. More specifically, one could simply represent the adjacency matrix as a big vector, and use standard machine learning techniques. Alternately, one could ignore vertex labels and compute a set of graph invariants (such as clustering coefficient). One could then classify using only these invariants. Neither of these

approaches use both vertex labels and graph structure. We demonstrate via proofs, simulation, analysis of a neurobiological data set (MR connectomes), and synthetic data analysis, that utilizing graph structure can significantly enhance one’s classification accuracy. However, the best approach for any particular data set is a function of both the amount of data and the true model. Moreover, even if the model were true, given a relatively small sample size, the estimated signal subgraph will often overlap with the truth, but not fully encapsulate it. Nonetheless, the below described classifiers still significantly outperform the benchmarks.

## 2 METHODS

### 2.1 Setting

Let  $\mathbb{G} : \Omega \mapsto \mathcal{G}$  be a graph-valued random variable with samples  $G_i$ . Each graph is defined by a set of  $V$  vertices,  $\mathcal{V} = \{v_i\}_{i \in [V]}$ , where  $[V] = \{1, \dots, V\}$ , and a set of edges between pairs of vertices  $\mathcal{E}$ , where  $|\mathcal{E}| \leq V^2$ . An adjacency matrix,  $A$ , is a binary  $V \times V$  matrix listing which vertices share an edge. Let  $Y : \Omega \mapsto \mathcal{Y}$  be a discrete-valued random variable with samples  $y_i$ . Assume the existence of a collection of  $n$  exchangeable samples of graphs and their corresponding classes from some true but unknown joint distribution:  $\{(\mathbb{G}_i, Y_i)\}_{i \in [n]} \stackrel{exch.}{\sim} F_{\mathbb{G}, Y}$ . Our aim (or exploitation task) is to build a graph classifier that could take a new graph,  $g$ , and correctly estimate its class,  $y$ , assuming that they are jointly sampled from the same distribution,  $F_{\mathbb{G}, Y}$ . Moreover, we are interested solely in graph classifiers that are *interpretable* with respect to the vertices and edges of the graph. In other words, manifold learning, feature extraction, and related approaches are inadmissible.

• J.T. Vogelstein and C.E. Priebe are with the Department of Applied Mathematics and Statistics, Johns Hopkins University, Baltimore, MD 21218.

E-mail: joshuav@jhu.edu

• W.R. Gray and R.J. Vogelstein are with the Johns Hopkins University Applied Physics Laboratory, Laurel, MD, 20723.

## 2.2 Model

A model defines the set of distributions under consideration. In the graph classification domain, we consider the model,  $\mathcal{F}_{\mathbb{G},Y}$ , which includes all joint distributions over graphs and classes under consideration:  $\mathcal{F}_{\mathbb{G},Y} = \{F_{\mathbb{G},Y}[\cdot; \theta] : \theta \in \Theta\}$ , where  $\theta \in \Theta$  indexes each distribution. Two “standard” approaches for tackling a classification problem are (i) the *generative* approach and (ii) the *discriminative* approach. In a generative strategy, one decomposes the joint distribution into a product of a likelihood term and a prior term:  $F_{\mathbb{G},Y} = F_{\mathbb{G}|Y}F_Y$ . In a discriminative strategy, one decomposes the joint distribution into a posterior term and a marginal term:  $F_{\mathbb{G},Y} = F_{Y|\mathbb{G}}F_{\mathbb{G}}$ . We proceed using a hybrid generative-discriminative approach whereby we describe a generative model and place constraints on the discriminant boundary.

First, assume that each graph has the same set of labeled vertices, so that all the variability in the graphs is in the adjacency matrix, which implies that  $F_{\mathbb{G},Y} = F_{A,Y}$ . Second, assume edges are independent, that is:  $F_{A,Y} = \prod_{u,v \in \mathcal{E}} F_{A_{uv},Y}$ . Now, consider the generative deconstruction, and let  $F[A_{uv}|Y = y] = f_{uv|y}$  and  $F_Y = \pi_Y$ . Third, assume the existence of a class-conditional difference, that is  $f_{uv|0} \neq f_{uv|1}$  for some  $(u, v) \in \mathcal{E}$ , and denote the edges satisfying that condition the *signal subgraph*,  $\mathcal{S} = \{(u, v) \in \mathcal{E} : f_{uv|0} \neq f_{uv|1}\}$ . Fourth, for concreteness, assume that the graphs are *simple* graphs, that is, undirected, with binary edges, and lacking (self-) loops. Thus, the likelihood of an edge between vertex  $u$  and  $v$  is given by a Bernoulli random variable with a scalar probability parameter:  $f_{uv|y} = \text{Bern}(A_{uv}; p_{uv|y})$ . Together, these four assumptions imply the following model:

$$\begin{aligned} \mathcal{F}_{\mathbb{G},Y} &= \{F_{A,Y}[a, y; \theta] : \theta \in \Theta\}, \text{ such that} \\ f_{A,Y}[a, y; \theta] &= \prod_{uv \in \mathcal{E} \setminus \mathcal{S}} \text{Bern}(a_{uv}; p_{uv|y}) \\ &\quad \times \prod_{uv \in \mathcal{S}} \text{Bern}(a_{uv}; p_{uv|y}) \pi_y, \quad (1) \end{aligned}$$

where  $\theta = \{p, \pi, \mathcal{S}\}$ . The likelihood parameter,  $p = \{p_{uv|y}\}_{uv \in \mathcal{E}, y \in \mathcal{Y}}$ , is constrained such that each term must be between zero and one:  $p_{uv|y} \in (0, 1)$ . The prior parameter,  $\pi = \{\pi_y\}$ , must be greater than or equal to zero and sum to one:  $\pi_y \geq 0, \sum_y \pi_y = 1$ . The signal subgraph parameter is a non-empty subset of the set of possibly edges,  $\mathcal{S} \subseteq \mathcal{E} \cap \mathcal{S} \neq \emptyset$ .

Note that given a specification of the class-conditional likelihood of each edge and class-prior, one completely defines a possible joint distribution over graphs and classes; the signal subgraph is implicit in that parameterization. However, the likelihood parameters for all edges not in the signal subgraph,  $p_{uv|y} = p_{uv} \forall y \in \mathcal{Y}, (u, v) \notin \mathcal{S}$ , are *nuisance* parameters; that is, they contain no class-conditional signal. In other words, when computing a relative

posterior class estimate, these nuisance parameters cancel in the ratio.

## 2.3 Classifier

Formally, we say that a graph classifier,  $h \in \mathcal{H}$ , is any function satisfying  $h : \mathcal{G} \mapsto \mathcal{Y}$ . We desire to obtain the “best” possible classifier,  $h_*$ . To define best, we first define a loss function,  $\ell_h : \mathcal{G} \times \mathcal{Y} \mapsto \mathbb{R}_+$ , specifically the 0 – 1 loss function:

$$\ell_h(G, Y) \triangleq \mathbb{I}\{h(G) \neq Y\}, \quad (2)$$

where  $\mathbb{I}\{\cdot\}$  is the identity function, equaling one whenever its argument is true, and zero otherwise. Further, let risk,  $R : \mathcal{F} \times \mathcal{H} \mapsto \mathbb{R}_+$  be the expected loss under the true distribution:

$$R(F, h) \triangleq \mathbb{E}_F[\ell_h(G, Y)]. \quad (3)$$

We define the best (optimal) classifier for a given distribution  $F$  as the one that minimizes risk. It can be shown that the classifier that maximizes the class-conditional posterior,  $F_{Y|\mathbb{G}}$  is optimal [3]:

$$\begin{aligned} h_*(G) &= \underset{h \in \mathcal{H}}{\text{argmin}} \mathbb{E}_F[\ell_h(G, Y)] = \underset{Y \in \mathcal{Y}}{\text{argmax}} F[Y|G] \\ &= \underset{Y \in \mathcal{Y}}{\text{argmax}} F[G|Y]F[Y]. \quad (4) \end{aligned}$$

Given the proposed model, Eq. (4) can be further factorized using the above four assumptions:

$$\underset{Y \in \mathcal{Y}}{\text{argmax}} F[G|Y]F[Y] = \underset{Y \in \mathcal{Y}}{\text{argmax}} \prod_{u,v \in \mathcal{S}} \text{Bern}(A_{uv}; p_{uv|y}) \pi_y. \quad (5)$$

Unfortunately Bayes optimal classifiers are typically unavailable. In such settings, it is therefore desirable to construct a classifier estimate from a set of *training data*. Formally, let  $\mathcal{T}_n$  denote the training corpus, assumed to be sampled exchangeably from the true but unknown distribution:  $\mathcal{T}_n = \{(\mathbb{G}_i, Y_i)\}_{i \in [n]} \stackrel{\text{exch.}}{\sim} F_{\mathbb{G},Y}$ . Given such a training corpus, and a new, as yet unclassified graph,  $g$ , an estimated classifier predicts the true (but unknown) class of  $g$  by utilizing the training corpus:  $\hat{h}_n : \mathcal{G} \times (\mathcal{G} \times \mathcal{Y})^n \mapsto \mathcal{Y}$ . When a model,  $\mathcal{F}_{\mathbb{G},Y}$  is specified, a beloved approach is to use a *Bayes plugin classifier*. Due to the above simplifying assumptions, the Bayes plugin classifier for this model is defined as follows. First, estimate the model parameters:  $\theta = \{\mathcal{S}, p, \pi\}$ . Second, plug those estimates into the above equation. The result is a Bayes plugin graph classifier:

$$\hat{h}_n(g) \triangleq \underset{y \in \mathcal{Y}}{\text{argmax}} \prod_{u,v \in \mathcal{S}} \hat{p}_{uv|y}^{a_{uv}} (1 - \hat{p}_{uv|y})^{(1-a_{uv})} \hat{\pi}_y, \quad (6)$$

where the Bernoulli probability is explicit. To implement such a classifier estimate, we specify estimators for  $\mathcal{S}$ ,  $\pi$  and  $p$ .

## 2.4 Estimators

In this section we describe estimators to estimate the estimands (parameters) of our model. An *estimator* is a function that maps from the multiple-sample space to the parameter space:  $\hat{\theta}_n : \Xi^n \mapsto \Theta$ ; the output of this function is called the *estimate*. In the graph classification domain, for example,  $\Xi = (\mathcal{G}, \mathcal{Y})$ . In a slight abuse of notation, we will also refer to the sequence of estimators,  $\hat{\theta}_1, \hat{\theta}_2, \dots$ , as an estimator. We desire (a sequences of) estimators that satisfy the following desiderata:

- **Consistent:** an estimator is consistent if its sequence converges in the limit to the true value:  $\lim_{n \rightarrow \infty} \hat{\theta}_n = \theta$ .
- **Efficient:** an estimator is efficient if its sequence converges to the minimum variance:  $\lim_{n \rightarrow \infty} \text{Var}(\hat{\theta}_n) = \mathcal{I}_\theta^{-1}$ . A maximally efficient estimator yields an estimate with *minimum variance*.
- **Robust:** an estimator is robust if the resulting estimate is relatively insensitive to small model misspecifications. Because the space of models is massive (uncountably infinite), it is intractable to consider all misspecifications, so we only consider a few of them below.
- **Quadratic complexity:** computational time complexity should be quadratic in the number of or less.
- **Interpretable:** we desire that the parameters are interpretable with respect to a subset of vertices and/or edges.

In addition to the above categorical desiderata, we also desire “nice” finite sample and empirical performance.

### 2.4.1 Signal Subgraph Estimators

Naïvely, one might consider a search over all signal subgraphs, plugging each one in to the classifier, and select the best performing signal subgraph. This strategy is intractable because the number of signal subgraphs scales super-exponentially with the number of vertices (see Figure 1, left panel). Specifically, the number of edges in a simple graph with  $V$  vertices is  $d_V = \binom{V}{2}$ , so the number of unique subgraphs is  $2^{\binom{V}{2}}$ . Searching over all of them is therefore ridiculously computationally taxing, failing the quadratic complexity criterium (it would even fail an exponential complexity criterium). We therefore consider several alternatives.

Before proceeding, recall that each edge is independent, which means that whether or not each edge is in the signal subgraph could be evaluated on its own (although not necessarily advisable, consider the Stein estimator [4]). Formally, consider a hypothesis test for each edge. The null hypothesis is that the class-conditional edge distributions are the same, so  $H_0 : f_{uv|0} = f_{uv|1}$  for all  $(u, v) \in \mathcal{S}$ . The composite alternative hypothesis is that they differ,  $H_A : f_{uv|0} \neq$

$f_{uv|1}$  for all  $(u, v) \in \mathcal{S}$ . Given such hypothesis tests, one can construct test statistics using the data:  $T \triangleq T_{uv}^{(n)} : \mathcal{T}_n \mapsto \mathbb{R}_+$ . We reject the null in favor of the alternative whenever the value of the test-statistic is greater than some critical-value:  $T(\mathcal{T}_n) > c$ . We can therefore construct a *significance matrix*:  $\mathbf{T} \triangleq T_{uv}^{(n)}$ , which is the sufficient statistic for the signal subgraph estimators.

#### 2.4.1.1 Incoherent Signal Subgraph Estimators:

Assume the size of the signal subgraph,  $|\mathcal{E}| = s$ , is known. The number of subgraphs with  $s$  edges on  $V$  vertices is given by  $\binom{d_V}{s}$ , where  $d_V$  is the number of distinct edges in a graph with  $V$  vertices; also super-exponential (see Figure 1, middle panel). Thus searching them all is currently computationally intractable. When  $s$  is given and the independent edge assumption is “good”, one can choose the critical value  $a$  *a posteriori* to ensure that only  $s$  edges are rejected,  $c = \min_{c'}!$  such that  $\sum_{(u,v) \in \mathcal{S}} \mathbb{I}\{T_{uv}^{(n)} < c'\} \geq s$ . Therefore, an estimate of the signal subgraph is the collection of  $s$  edges with minimal test-statistics. Formally, let  $T_{(1)} < T_{(2)} < \dots < T_{(d_V)}$  indicated the *ordered* test statistics (dropping the superscript indicating the number of samples for brevity). Then, the *incoherent signal subgraph estimator* is given by:  $\hat{\mathcal{S}}_n^{\text{inc}} = \{a_{(1)}, \dots, a_{(s)}\}$ , where  $a_{(u)}$  indicates the  $u^{\text{th}}$  edge ordered by significance of its test statistic,  $T_{(u)}$ .

**2.4.1.2 Coherent Signal Subgraph Estimators:** In addition to the size of the signal subgraph, also assume that each of the edges in the signal subgraph are incident to one of  $m$  special vertices called *star vertices*. While this assumption further constrains the candidate sets of edges, the number of feasible sets still scales super exponentially (see Figure 1, right panel). Instead, we again take a greedy approach.

First, compute the significance of each edge, as above, yielding ordered test-statistics, and rank edges by significance with respect to each vertex,  $E_{k,(1)} \leq E_{k,(2)} \leq \dots \leq E_{k,(n-1)}$  for all  $k \in \mathcal{V}$ . Second, recursively increase the critical value,  $c$ . With each iteration, assign each vertex a “score” equal to the number of edges incident to that vertex more significant than the critical value,  $w_{v;c} = \sum_{u \in [V]} \mathbb{I}\{T_{i,u} < c\}$ . If there exists  $m$  vertices whose scores sum to greater than or equal the size of the signal subgraph,  $s$ , then stop iterating. That is, find  $c = \min_{c'}!$  such that  $\sum_i w_{v;c'} \geq s$ . Call the collection of  $s$  most significant edges from within that subset the *incoherent signal subgraph estimate*,  $\hat{\mathcal{S}}_n^{\text{coh}}$ .

**2.4.1.3 Coherograms:** In the process of estimating the incoherent signal subgraph, one builds a “coherogram”. Each row of the coherogram corresponds to a different critical value  $c$ , and each column corresponds to a different vertex  $v$ . The  $(c, v)^{\text{th}}$  element of the coherogram is the number of edges incident to vertex  $v$  with significance smaller than  $c$ ,  $w_{v;c}$ . Thus, the coherogram gives a visual depiction of how coherent is the signal subgraph.

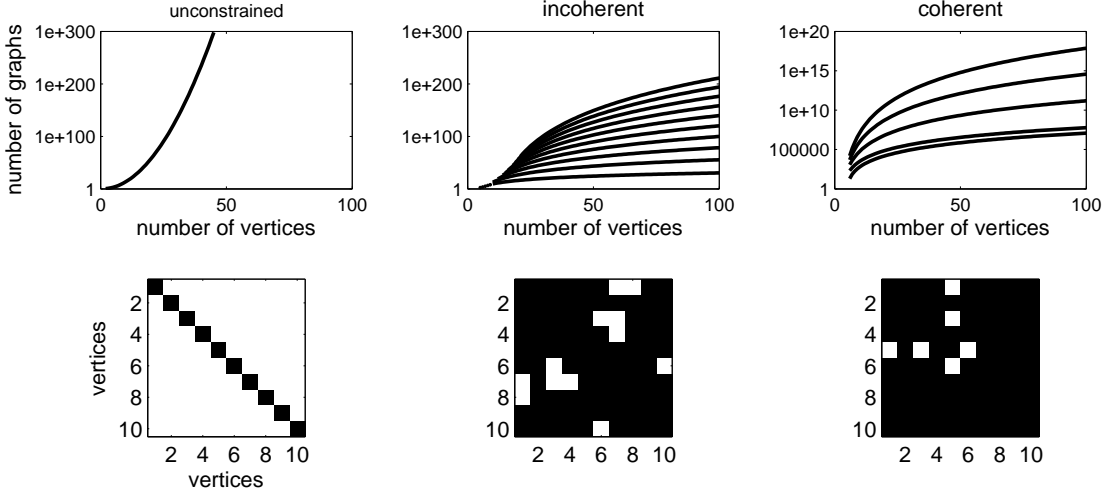


Fig. 1. Exhaustive searches for the signal subgraph, even given severe constraints, are computationally intractable for small graphs (e.g., with  $\mathcal{O}(10)$  vertices). Top panels show the number of unique simple subgraphs as a function of the number of vertices,  $V$ . Note the ordinates are all log scale. On the left is the unconstrained scenario, that is, all possible subgraphs for a given number of vertices. In the middle panel, each line shows the number of subgraphs with fixed number of edges,  $s$ , ranging from 10 to 100, incrementing by 10 with each line. The right panel shows the number of subgraphs for various fixed  $s$  and only a single star-vertex, that is, all edges are incident to one vertex. Bottom panels show a particular example subgraph via its adjacency matrix; white elements indicate an edge.

#### 2.4.2 Likelihood Estimators

The class-conditional likelihood parameters,  $p_{uv|y}$ , are relatively simple. In particular, because the graphs are assumed to be simple,  $p_{uv|y}$  is just an independent Bernoulli parameter for each edge in each class. The maximum likelihood estimator (MLE), which simply the average value of each edge per class, is a principled choice:

$$\hat{p}_{uv|y}^{MLE} = \frac{1}{n_y} \sum_{i|y_i=y} a_{uv}^{(i)}, \quad (7)$$

where  $\sum_{i|y_i=y}$  indicates the sum is over all data samples from class  $y$ . Unfortunately, the MLE has relatively poor finite sample properties. In particular, if the data contains no examples of an edge in a particular class, then the MLE will be zero. If the unclassified graph exhibits that edge, then the probability of it being from that class is zero, which is undesirable. We therefore consider an estimator with better finite sample performance:

$$\hat{p}_{uv|y} = \begin{cases} \eta_n & \text{if } \max_i a_{uv}^{(i)} = 0 \\ 1 - \eta_n & \text{if } \min_i a_{uv}^{(i)} = 1 \\ \hat{p}_{uv|y}^{MLE} & \text{otherwise} \end{cases} \quad (8)$$

where we let  $\eta_n = 1/(10n)$ . The above estimator converges asymptotically to  $\hat{p}_{uv|y}^{MLE}$ , and therefore shares the MLE's asymptotical properties. Moreover, the above estimator is an L-estimator of  $p_{uv|y}$ , and therefore shares the robustness properties of L-estimators [5]

#### 2.4.3 Prior Estimators

The prior are the simplest. The prior probabilities are Bernoulli, and we are only concerned with the case where  $|\mathcal{Y}| \ll n$ , so the maximum likelihood estimators are sufficient:

$$\hat{\pi}_y = \frac{n_y}{n}, \quad (9)$$

where  $n_y = \sum_{i \in [n]} \mathbb{I}\{y_i = y\}$ .

### 2.5 Evaluation Criteria

The properties of the MAP and ML estimators for the likelihood and prior terms, respectively, are well studied [3] and will therefore not be discussed in much detail.

#### 2.5.1 Classifier

We evaluate the classifier finite sample properties using either hold-out or leave-one-out misclassification performance, depending on whether the data is simulated or experimental, respectively. Formally, given  $C$  equally sized subsets of the data:  $\{\mathcal{T}_1, \dots, \mathcal{T}_C\}$ , the cross-validated error is:

$$\hat{L}_{\hat{h}(\cdot; \mathcal{T}_n)} = \frac{1}{C} \sum_{c=1}^C \frac{1}{|\mathcal{T}_n \setminus \mathcal{T}_c|} \sum_{g \notin \mathcal{T}_c} \mathbb{I}\{\hat{h}(g; \mathcal{T}_c) \neq y\}. \quad (10)$$

Given this definition, let  $L_{\hat{\pi}}$  be the classifier using only the prior estimates, and let  $L_*$  be the error for the Bayes optimal classifier.

To determine whether a classifier is significantly better than chance, we randomly permute the classes



Fig. 2. An example of the coherent signal subgraph estimate’s improved accuracy over the incoherent signal subgraph estimate, for a particular homogeneous two-class model specified by:  $\mathcal{M}_{70}(1, 20; 0.5, 0.1, 0.3)$ . Each row shows the same columns but for increasing the number of graph/class samples. The columns show the: (far left) negative log-significant matrix, computed using Fisher’s exact test (lighter means more significant; each panel is scaled independent of the others because only relative significance matters here); (middle left) incoherent estimate of the signal subgraph; (middle right) coherent estimate of the signal subgraph; (far right) coherogram. As the number of data samples increases (lower rows), both the incoherent and coherent estimates converge to the truth (the ordinate labels of the middle panels indicate the number of edges correctly identified). For these examples, the coherent estimator tends to find more true edges. The coherogram visually depicts the coherency of the signal; it is also converging to the truth—the signal subgraph here contains a single star-vertex.

of each graph  $n_{MC}$  times, and then estimate a naïve Bayes classifier using the permuted data, yielding an empirical distribution. The p-value of a permutation test is the minimum fraction of Monte Carlo permutations that did better than the classifier of interest [6].

To determine whether a pair of classifiers are significantly different, we compare the leave-one-out classification results using McNemar’s test [7]

### 2.5.2 Signal Subgraph Estimators

To evaluate absolute performance of the signal subgraph estimators, we define here “miss-edge rate”

as the fraction of true edges missed by the signal subgraph estimator:

$$R_n^x = \frac{1}{S} \sum_{(u,v) \in S} \mathbb{I}\{(u,v) \in \hat{S}_n^x\} \quad (11)$$

Further, we estimate the *relative rate* and *relative efficiency* to evaluate the relative finite sample properties of a pair of consistent estimators. The relative rate is simply  $(1 - R_n^{inc})/(1 - R_n^{coh})$ . Relative efficiency is relative number of samples for the coherent estimator to obtain the same rate as the incoherent estimator.

### 3 RESULTS

The Results section is subdivided into three subsections, corresponding to asymptotic properties, finite sample properties, and performance on connectome data.

#### 3.1 Asymptotic properties

##### 3.1.1 Likelihood and Prior term Estimators

MAP estimators are known to be consistent and efficient, both for finite samples and asymptotically, under certain special cases. Specifically, letting  $d_V = \binom{V}{2}$  (the number of edges in a simple graph as a function of the number of vertices,  $V$ ), and assuming  $n \rightarrow \infty$  and  $V$  is fixed, we know that:  $\hat{p}_{uv|y}^{MAP} \rightarrow p_{uv|y}$  [8]. The MAP estimator remains consistent when  $V \rightarrow \infty$  as long as  $d_V/V \rightarrow 0$  [3]. Moreover, both prior and likelihood estimates are trivial to compute, as closed-form analytic solutions are available for both.

##### 3.1.2 Signal Subgraph Estimators

A variety of test-statistics are available for computing the edge-specific class-conditional signal,  $T_{uv}^{(n)}$ . Which ever test one uses, the sufficient statistics are encapsulated in a  $|\mathcal{Y}|$  by two contingency table, indicating the number of edges observed in each class. For example, the two-class contingency table for each edge is:

	Class 0	Class 1	Total
Edge	$n_{uv 0}$	$n_{uv 1}$	$n_{uv}$
No Edge	$n_0 - n_{uv 0}$	$n_1 - n_{uv 1}$	$n - n_{uv}$
Total	$n_0$	$n_1$	$n$

Fisher's exact test computes the probability of obtaining a table equal to or more extreme than the table resulting from the null hypothesis: that the two classes have the same probability of sampling an edge. In other words, Fisher's exact test is the most powerful statistical test assuming independent edges [8]. Furthermore, whenever  $p_{uv|0} \neq p_{uv|1}$ , the p-value of Fisher's exact test converges to zero; whereas whenever  $p_{uv|0} = p_{uv|1}$ , the distribution of p-values converges to the uniform distribution between zero and one. Therefore, Fisher's exact test is a consistent estimator as  $n \rightarrow \infty$ , assuming a fixed and finite  $V$ . Moreover, as  $V \rightarrow \infty$ , as long as  $V/n \rightarrow 0$ , Fisher's exact test remains consistent [8]. While most powerful, computing Fisher's exactly is computationally taxing. Fortunately, the chi-squared test is asymptotically equivalent to Fisher's test, and therefore shares those convergence properties [8]. Even the absolute difference of MAP estimates,  $|\hat{p}_{uv|1}^{MAP} - \hat{p}_{uv|0}^{MAP}|$ , which is trivially easy to compute, is asymptotically equivalent to Fisher's [8] and therefore consistent.

The implications of the above convergence properties are that any incoherent signal subgraph estimated using a consistent test-statistic is a consistent

signal subgraph estimator. Moreover, the incoherent signal subgraph estimator is robust to a variety of model misspecifications. Specifically, as long as all the marginal probability of all the edges in the signal subgraph are different between the two classes,  $p_{uv|1} \neq p_{uv|0}$ , any consistent test-statistic will yield a consistent signal subgraph. For example, when the signal subgraph is coherent, even if  $m$  is unknown, the incoherent signal subgraph estimator will converge to the truth.

Moreover, the coherent signal subgraph estimator uses the same test-statistics. Thus, it shares the above consistency and robustness properties. Estimating the coherent signal subgraph is more computationally time consuming. What is lost by computational time, however, is typically gained by finite sample efficiency whenever the model is coherent, as will be shown below.

##### 3.1.3 Bayes plugin classifier

A Bayes plugin classifier is a consistent classifier whenever the estimates that are plugged in are consistent [3]. Because the likelihood, prior, and signal subgraph estimates are all consistent, the Bayes plugin classifier is therefore consistent as well. Moreover, it is well-known that a naïve Bayes classifier often exhibits impressive finite sample performance due to it winning the bias-variance trade-off relative to other classifiers [9]. In other words, even when edge are highly dependent, because marginal probability estimates are more efficient than joint probability estimates, an independent edge based classifier will often outperform a classifier based on dependencies.

#### 3.2 in simulo experiments

To better assess the finite sample properties of the signal subgraph estimators, we conduct a number of in simulo experiments. First, consider the following *homogeneous* model: each simple graph has  $V = 70$  vertices. Class 0 graphs are Erdos-Renyi with probability  $p$  for each edge, that is:  $f_{uv|0} = p \forall (u, v) \in \mathcal{E}$ . Class 1 graphs are a mixture of two Erdos-Renyi models: all edges in the *signal subgraph* have probability  $q$ , and all others have probability  $p$ :  $f_{uv|1} = q \forall (u, v) \in \mathcal{S}$ , and  $f_{uv|1} = p \forall (u, v) \in \mathcal{E} \setminus \mathcal{S}$ . The signal subgraph is constrained to have  $m$  star-vertices and  $s$  edges. The prior probability of being in class 0 is  $\pi$ , so  $1 - \pi$  is the probability of coming from class 1. Thus, the model is characterized by  $F_\theta = \mathcal{M}_V(m, s; \pi, p, q)$ , where  $V$  is a constant,  $m$  and  $s$  are hyper-parameters, and  $\pi$ ,  $p$  and  $q$  are parameters. To evaluate the finite sample performance of the two above-described signal subgraph estimators for this model, we run some numerical experiments, with results provided in Figure 2. In each row, we sample  $n/2$  graphs from each class defined by  $\mathcal{M}_{70}(1, 20; 0.5, 0.1, 0.3)$ . Given these  $n$  samples, we compute the significance matrix

(first column), which contains the sufficient statistics for both estimators. The incoherent estimator simply chooses the  $s$  most significant edges as the signal subgraph (second column). The coherent estimator first guesses which are the  $m$  star-vertices, and then chooses the  $s$  most significant edges incident to at least one of those vertices (third column). The coherogram shows how “coherent” is the signal from the data (fourth column).

From this figure, one might notice a few tendencies. First, both the incoherent and coherent signal subgraph estimators are converging relatively quickly towards the true signal subgraph. Second, while the coherent estimator struggles with relatively little data, it seems to converge more quickly than the incoherent estimator. Third, the coherogram sharpens with additional samples, clearly showing that this model is strongly coherent after about only 50 samples.

To better characterize the relative performance of the two signal subgraph estimators, Figure 3 shows their performance as a function of the number of samples,  $n$ , for this model. The top panel shows the mean and standard error of the missed-edge rate: the fraction of edges incorrectly identified. For essentially all  $n$ 's, the coherent estimator (black line) performs better than the incoherent estimator (gray line). This translates directly to improved classification performance (lower panel), where the plugin classifier using the coherent signal subgraph classifier (black line) has a better misclassification rate than the incoherent signal subgraph classifier (dark gray line) for essentially all  $n$ . For comparison purposes, the naïve Bayes plugin classifier, that is, the classifier that assumes the whole graph is the signal subgraph, is also shown (light gray line). Note that the performance of all the classifiers is bounded above by  $L_{\hat{\pi}} = 0.5$  and below by  $L_* = 0.13$ . Moreover,  $\hat{L}_{nb} \geq \hat{L}_{inc} \geq \hat{L}_{coh} \geq L_*$  for essentially all  $n$  here.

### 3.3 Relative Efficiency

The above numerical results suggest that the coherent estimator outperforms the incoherent estimator most of the time. However, that result is a function of both the model,  $\mathcal{M}_V$  (which includes the number of vertices), and the number of samples  $n$ . Figure 4 explicitly shows that the relative performance of an estimator for a particular model changes as a function of the number of samples. More specifically, for small  $n$ , the incoherent estimator yields a better performance, as indicated by by relative rate and relative efficiency being above one. However, with more samples, when the signal subgraph is coherent, the coherent estimator will eventually outperform the incoherent one. At infinite samples, since both estimators are consistent, they will yield identical results: the truth.

Thus, to choose which estimator will likely achieve best, knowledge of the model,  $\mathcal{M}_V(m, s; \pi, p, q)$ , is

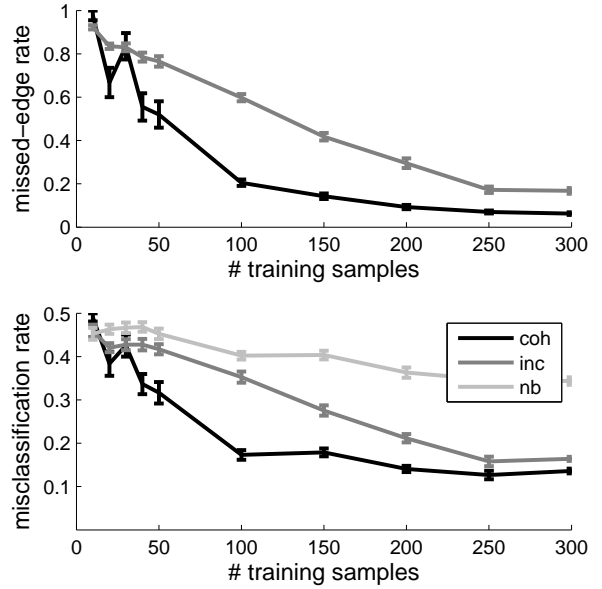


Fig. 3. Performance statistics as a function of sample size demonstrate that the coherent signal subgraph estimator outperforms the incoherent signal subgraph estimator, in terms of both the signal subgraph identification and classification, for nearly all  $n$ , using the same model as in Figure 2. The top panel shows the missed-edge rate for each estimator as a function of the number of training samples,  $n$ . The bottom panel shows the corresponding misclassification rate for the two estimators, as well as the naïve Bayes plugin classifier. Performance of all estimators increases (nearly) monotonically with  $n$  for both criteria. Error bars show standard error of the mean here and elsewhere (averaged over 20 trials; each trial used 100 samples for held-out data). Note that for most values of  $n$ , we have  $L_{\hat{\pi}} \geq \hat{L}_{nb} \geq \hat{L}_{inc} \geq \hat{L}_{coh} \geq L_*$ .

insufficient; rather, both the model and the number of samples must be known a priori.

### 3.4 Estimating the hyper-parameters

In the above analyses the hyper-parameters, both the number of edges  $s$  and star-vertices  $m$ , were known. In practice while one might have a preliminary guess of the range of these hyper-parameters, they will at times be unknown. We can therefore use a cross-validation technique to search over the space of all reasonable combinations of  $s$  and  $m$ , and choose the best performing combination. Figure 5 shows one such simulation depicting several key features. The top panel shows the misclassification rate as a function of the log of the size of the signal subgraph,  $s$ . Although the true size is  $s = 20$ , the best performing estimate is  $\hat{s} = 23$ . This is a relatively standard result in model selection: the best performer will include a few extra dimensions because adding a few

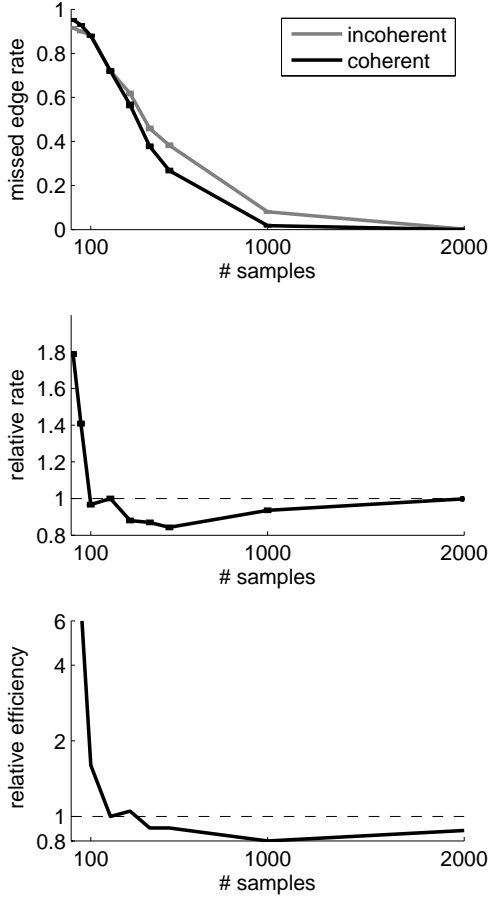


Fig. 4. The relative performance of the coherent and incoherent estimators is a function not just of the model, but also the number of samples. Specifically, for the model  $\mathcal{M}_{30}(1, 5; 0.5, 0.1, 0.2)$ , we compute the missed-edge rates for both the incoherent estimator (gray line) and the coherent estimator (black line). The top panel shows that for small sample size the incoherent estimator achieves a better (lower) missed-edge rate than the coherent estimator. However, the incoherent estimator’s convergence rate is slower, therefore, the coherent estimator catches up and outperforms the incoherent estimator; until both eventually converge at the truth. The middle and bottom panels show the relative rate and efficiency curves for this model. Note that they dip below unity, and then converge back up to unity, as they must because both estimators are consistent.

uninformative features is less costly than missing a few informative features [10]. This intuition is further reified by the U-shape of the misclassification curve on a log scale: including many non-signal edges is less detrimental than excluding a few signal edges.

The bottom panel shows the performance by varying both  $m$  and  $s$ , which has a “banded” like structure, indicating that the performance is relatively robust to small changes in  $m$ . Moreover, the best performing pair achieved  $\hat{L}_{coh} = 0.13$  with  $\hat{m} = 1$  and  $\hat{s} = 24$ , suggesting that  $n$  was sufficiently large to correctly find the true star-vertex, and further corroborating the “better safe than sorry” attitude to selecting the signal vertices.

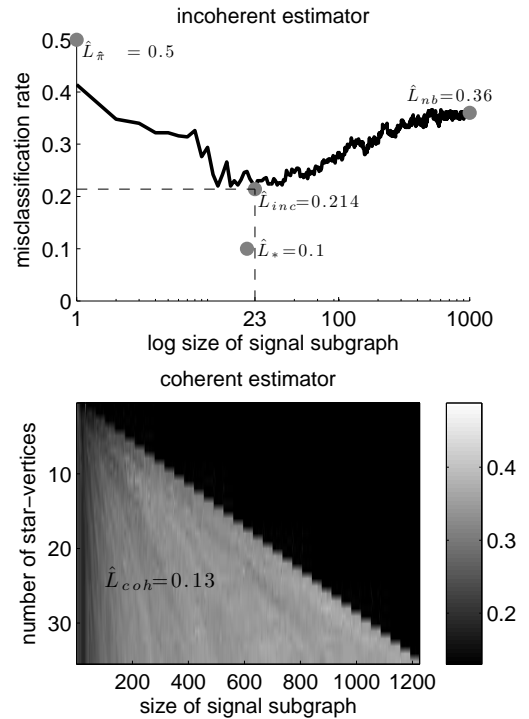


Fig. 5. When constraints on the number of edges ( $s$ ) or star-vertices ( $m$ ) are unknown, a search over these hyperparameters can yield estimates  $\hat{s}$  and  $\hat{m}$ . Both panels depict held-out cross-validation error as a function of varying these parameters for the same model as in Figure 4, using 200 training samples and 500 test samples, with  $m = 1$  and  $s = 20$ . The top panel depicts misclassification rate of the incoherent estimator as a function of the number of edges on a log scale. Note that in this simulation, while  $s = 20 < \hat{s}_{inc} = 23$ . This “conservatism” is typical and appropriate in many model selection situations. The bottom panel shows  $\hat{L}_{coh}$  as a function of both  $m'$  and  $s'$ . For this simulation,  $\hat{m} = 1$  and  $\hat{s} = 24$ , further corroborating the conservative stance on model selection. Note that  $L_{\pi} \geq \hat{L}_{nb} \geq \hat{L}_{inc} \geq \hat{L}_{coh} \geq L_{*}$  as one would hope for this coherent simulation.



### 3.5 MR Connectome Classification

A connectome may be defined as the complete set of connections of the brain [11]. MR connectomes utilize multi-modal Magnetic Resonance (MR) imaging to determine both the vertex and edge set for each individual [2]. This section investigates the utility of the above described classifiers on data collected for the Baltimore Longitudinal Study on Aging, as described previously [12]. Briefly, 49 subjects (25 male, 24 female) underwent a DTI protocol, simple graphs with 70 vertices (each vertex corresponding to a neuroanatomical region as defined by [13]) were estimated using the MRCAP layout [14]. Lacking strong priors on either the number of edges or star-vertices in the signal subgraph (or even whether a signal subgraph existed), we searched over a large space of hyper-parameters using cross-validated misclassification performance as our metric of success (Figure 6). The naïve Bayes classifier—which assumes the signal subgraph is the whole edge set,  $\hat{S}_{nb} = \mathcal{E}$ —performs marginally better than chance:  $\hat{L}_{nb} = 0.39$  (p-value  $\approx 0.05$  assessed by a permutation test). With a relatively small number of incoherent edges— $\hat{s}_{inc} = 10$ —the incoherent classifier (top left panel) achieves  $\hat{L}_{inc} = 0.27$ , significantly better than chance (p-value  $< 0.0007$ ), but not significantly better than the naïve Bayes classifier (using McNemar’s test). The coherent classifier achieved a minimum of  $\hat{L}_{coh} = 0.18$  (top right and middle panels), not significantly better than the incoherent classifier, but significantly better than both chance and the naïve Bayes classifier (p-values  $< 10^{-5}$  and  $< 0.004$ , respectively; note that no multiple hypothesis testing corrections were performed). This improved performance upon using the coherent classifier suggests that signal subgraph is coherent. Using  $\hat{m}_{coh} = 12$  and  $\hat{s}_{coh} = 360$  from the best performing coherent classifier, we can estimate the signal subgraph (bottom right). The coherogram suggests that indeed, the signal is somewhat, but not strikingly coherent (bottom right).

### 3.6 Model Evaluation

Although the above coherent classifier estimated a signal subgraph, we wondered to what extent can we believe that it is the true signal subgraph. We address this question in two ways: (i) synthetic data analysis and (ii) assumption checking.

#### 3.6.1 Synthetic data analysis

For the synthetic data analysis, we generated some synthetic data as follows. Given the above estimated signal subgraph, for every edge not in  $\hat{S}_n$ , let  $p_{uv|0} = p_{uv|1} = \hat{p}_{uv}$ , where  $\hat{p}_{uv}$  is the estimated edge probability averaging over all samples. For all edges in  $\hat{S}_n$ , let  $p_{uv|y} = \hat{p}_{uv|y}$ . Set the priors according to the data as well:  $\pi = \hat{\pi}$ .

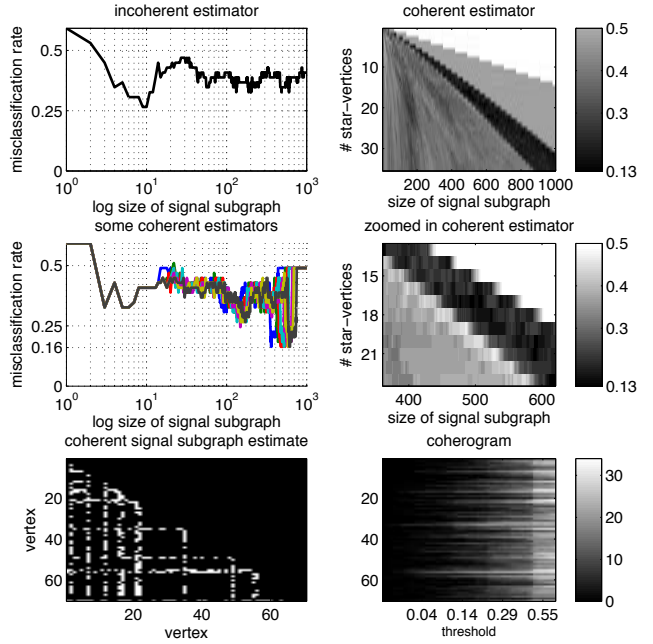


Fig. 6. MR connectome gender signal subgraph estimation and analysis. By cross-validating over hyper-parameters and models, we estimate that the “best” incoherent signal subgraph (for this inference task on these data) has  $\hat{s}_{inc} = 10$  and yields a misclassification rate of  $\hat{L}_{inc} = 0.27$ , whereas the best coherent signal subgraph has  $\hat{m}_{coh} = 12$  and  $\hat{s}_{coh} = 360$ , achieving  $\hat{L}_{coh} = 0.18$ . The top two panels depict the same as Figure 5. The middle two depict misclassification rate (left) for a few different choices of  $m'$  as a function of  $s'$  and (right) a zoomed in depiction of the top right panel. The bottom left panel shows the estimated signal subgraph, and the bottom right shows the coherogram. Together, these bottom panels suggest that the signal subgraph for these data is neither particularly coherent or incoherent.

Given this synthetic data model, we first sampled 49 training samples, 25 from class 0 and 24 from class 1, and estimated the incoherent and coherent classifier performance on this single trial (Figure 7, top panels). The performance of the classifiers on the synthetic data qualitatively mirrors that of the real data, suggesting some model goodness-of-fit. To assess what fraction of the edges in the estimated signal subgraph we could trust, even assuming the model was true, we then sampled up to 100 training samples (and 100 test samples), and computed the missed-edge rate (bottom left) and misclassification rate (bottom right) as a function of the number of samples. Given approximately 50 samples, the incoherent signal subgraph estimator correctly identifies about 40% of the edges, whereas the coherent signal subgraph estimator correctly identifies about 50%. This suggests that even if the model were true (which it is not) we should only believe that about half the edges

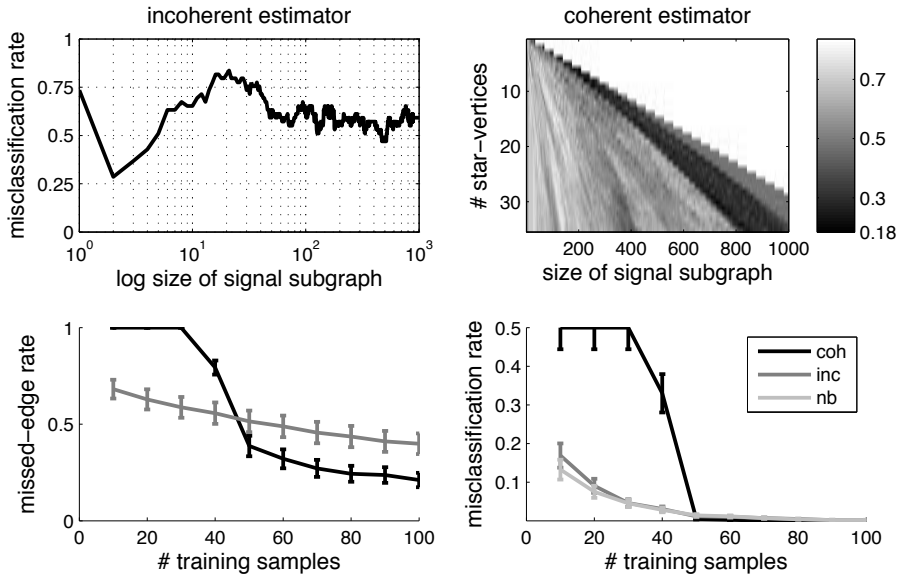


Fig. 7. Synthetic data analysis provides some intuition with model checking and improvement. The top two panels show the incoherent (left) and coherent (right) misclassification rates as a function of the hyper-parameter choices. These plots look quite similar to those from Figure 6, which is suggestive of an adequate model. The bottom panels show the missed-edge rate (left) and misclassification rate (right) as a function of number of training samples. With about 50 training samples, approximately half of the edges identified by either classifier are true edges. Moreover, more than 50 training samples seems to be sufficient for obtaining nearly perfect classification, suggesting perhaps only a few more subjects would be sufficient to yield much greater classification performance.

in the estimated signal subgraph are in the actual signal subgraph. Moreover, both missed-edge rate and misclassification rate exhibit a step-like function in performance: after about 50 samples, performance dramatically increases. This suggests that perhaps only a few more data points would be necessary to obtain near perfect classification accuracy.

### 3.6.2 Model checking

Checking whether edges are independent is relatively easy. Figure 8 shows the correlation coefficient between all pairs of edges in the estimated signal subgraph from the real data. For visualization purposes, we used a spectral clustering algorithm [15], with hopes that it would more clearly highlight any significant correlations. Several groups of edges seem to be highly correlated. To assess significance, we compare the distribution of correlation coefficients with the distribution of correlation coefficients obtained from the synthetic data analysis. A two-sample Kolmogorov-Smirnov test shows that the two matrices are significantly different ( $p$ -value  $\approx 0$ ), rejecting the null hypothesis that the edges in the real data are independent.

## 4 DISCUSSION

This work makes the following contributions. First, it introduces a novel graph/class model that admits

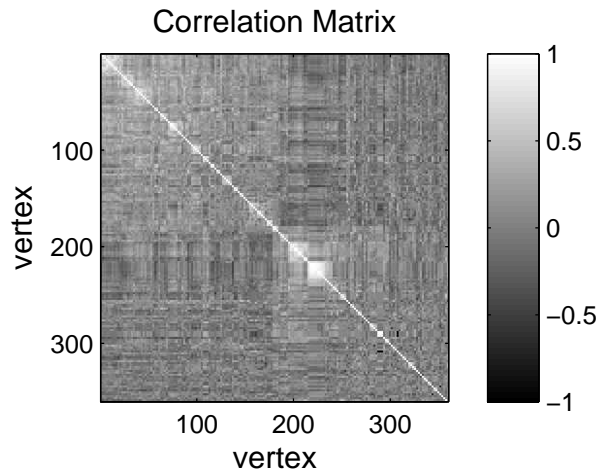


Fig. 8. The correlation matrix between all the edges in the coherent signal subgraph estimate. Edges are organized by co-clustering to highlight any similarities. Although most edges are uncorrelated, several groups of edges cluster, indicative of the fact that the edges are not independent ( $p$ -value of  $\approx 0$  using a two-sample Kolmogorov-Smirnov test comparing the real and synthetic correlation matrices).

rigorous statistical investigation. Moreover, it presents two approaches for estimating the signal subgraph: the first using only vertex label information, the second also utilizing graph structure. The resulting estimators have desirable asymptotic and finite sample properties, including consistency and robustness to various model misspecifications. Third, simulated data analysis indicate that neither approach dominates over the other; rather, which approach to use is a function of both the model and the amount of data. Fourth, these classifiers are applied to a connectome data set; the coherent classifier performs significantly better than both naïve Bayes and incoherent classifiers. Fifth, synthetic data analysis suggests that while we can use the signal subgraph estimators to improve classification performance, we should not expect that all the edges in the estimated signal subgraph will be the true signal edges, even when the model is correct. Moreover, we could expect a drastic performance boost by only a few additional data samples. Finally, model checking suggests that the independent edge assumption does not fit the data well.

Collectively, the above analyses suggest a number of possible next steps. First, one could collect more data. Second, one could relax the independent edge assumption, for instance, by considering conditionally independent edges [16]. Third, a number of conjectures have arisen due to these results. For instance, perhaps the misclassification rate is a monotonic function of the missed-edge rate. Fourth, improved classification performance could be achieved by (Bayesian) model-averaging to combine estimated signal subgraphs instead of picking one. Finally, all this work assumed binary edges and labeled vertices. Both of these assumptions could be relaxed.

We hope the proposed approaches will yield many applications. To that end, all the data and code used in this work is available from the author's website, [jovo.me](http://jovo.me).

## ACKNOWLEDGMENTS

## REFERENCES

- [1] H. Bunke and K. Riesen, "Towards the Unification of Structural and Statistical Pattern Recognition," *Pattern Recognition Letters*, vol. in press, 2011. [Online]. Available: <http://www.sciencedirect.com/science/article/pii/S0167865511001309>
- [2] P. Hagmann, L. Cammoun, X. Gigandet, S. Gerhard, P. Ellen Grant, V. Wedeen, R. Meuli, J. P. Thiran, C. J. Honey, and O. Sporns, "MR connectomics: Principles and challenges," *J Neurosci Methods*, vol. 194, no. 1, pp. 34–45, 2010. [Online]. Available: [http://www.ncbi.nlm.nih.gov/entrez/query.fcgi?cmd=Retrieve&db=PubMed&dopt=Citation&list\\_uids=20096730](http://www.ncbi.nlm.nih.gov/entrez/query.fcgi?cmd=Retrieve&db=PubMed&dopt=Citation&list_uids=20096730)
- [3] P. J. Bickel and K. A. Doksum, *Mathematical Statistics: Basic Ideas and Selected Topics, Vol I (2nd Edition)*. Prentice Hall, 2000. [Online]. Available: <http://www.amazon.com/Mathematical-Statistics-Basic-Selected-Topics/dp/013850363X>

- [4] C. M. Stein, "Inadmissibility of the usual estimator of the mean of a multivariate normal distribution," in *Proceedings of the Third Berkeley Symposium on Mathematical Statistics and Probability*, vol. 1. University of California Press, 1956, pp. 197–206.
- [5] P. J. Huber, *Robust Statistics*, ser. Wiley Series in Probability and Statistics. Wiley, 1981, vol. 82, no. 3. [Online]. Available: <http://doi.wiley.com/10.1002/9780470434697>
- [6] R. A. Fisher, *The Design of Experiments*. Macmillan Pub Co, 1971. [Online]. Available: <http://www.amazon.com/Design-Experiments-Ronald-Fisher/dp/0028446909>
- [7] Q. McNemar, "Note on the sampling error of the difference between correlated proportions or percentages," *Psychometrika*, vol. 12, no. 2, pp. 153–157, Jun. 1947. [Online]. Available: <http://www.springerlink.com/content/843g84t135765212/>
- [8] J. A. Rice, *Mathematical statistics and data analysis*, O. Barndorff-Nielsen, P. J. Bickel, W. S. Cleveland, and R. M. Dudley, Eds. Duxbury Press, 1995. [Online]. Available: <http://www.citeline.org/user/tarjeiha/article/1691927>
- [9] D. J. Hand and K. Yu, "Idiot's Bayes: Not So Stupid after All?" *International Journal Statistical Review*, vol. 69, no. 3, pp. 385–398, Nov. 2001. [Online]. Available: <http://www.jstor.org/pss/1403452>
- [10] a.K. Jain and P. Duin, "Statistical pattern recognition: a review," *IEEE Transactions on Pattern Analysis and Machine Intelligence*, vol. 22, no. 1, pp. 4–37, 2000. [Online]. Available: <http://ieeexplore.ieee.org/lpdocs/epic03/wrapper.htm?arnumber=824819>
- [11] O. Sporns, *Networks of the Brain*. The MIT Press, 2010. [Online]. Available: <http://www.amazon.com/Networks-Brain-Olaf-Sporns/dp/0262014696>
- [12] J. T. Vogelstein, W. R. Gray, J. L. Prince, L. Ferrucci, S. M. Resnick, C. E. Priebe, and R. J. Vogelstein, "Graph-Theoretical Methods for Statistical Inference on MR Connectome Data," *Organization Human Brain Mapping*, 2010.
- [13] R. S. Desikan, F. Ségonne, B. Fischl, B. T. Quinn, B. C. Dickerson, D. Blacker, R. L. Buckner, A. M. Dale, R. P. Maguire, B. T. Hyman, M. S. Albert, and R. J. Killiany, "An automated labeling system for subdividing the human cerebral cortex on MRI scans into gyral based regions of interest." *NeuroImage*, vol. 31, no. 3, pp. 968–80, Jul. 2006. [Online]. Available: <http://www.ncbi.nlm.nih.gov/pubmed/16530430>
- [14] W. R. Gray, J. A. Bogovic, J. T. Vogelstein, B. A. Landman, J. L. Prince, and R. J. Vogelstein, "Magnetic Resonance Connectome Automated Pipeline," *submitted*, 2010.
- [15] I. S. Dhillon, "Co-clustering documents and words using bipartite spectral graph partitioning," *Proceedings of the seventh ACM SIGKDD international conference on Knowledge discovery and data mining KDD 01*, vol. pages, no. April 2006, pp. 269–274, 2001. [Online]. Available: <http://portal.acm.org/citation.cfm?doid=502512.502550>
- [16] P. D. Hoff, A. E. Raftery, and M. S. Handcock, "Latent Space Approaches to Social Network Analysis," *Journal of the American Statistical Association*, vol. 97, no. 460, pp. 1090–1098, 2002.

PLACE  
PHOTO  
HERE

**Joshua T. Vogelstein** Joshua T. Vogelstein is a spritely young man, engorged in a novel post-buddhist metaphor.

**William R. Gray** William R. Gray graduated from Vanderbilt University in 2003 with a Bachelors degree in electrical engineering, and received his MS in electrical engineering in 2005 from the University of Southern California. Currently, Will is a PhD student in electrical engineering at The Johns Hopkins University, where he is conducting research in the areas of connectivity, signal and image processing, and machine learning. He is also a member of the technical staff at the Johns Hopkins University Applied Physics Laboratory, where he manages projects in the Biomedicine and Undersea Warfare business areas. Will is a member of IEEE, Eta Kappa Nu, and Tau Beta Pi

**R. Jacob Vogelstein** R. Jacob Vogelstein received the Sc.B. degree in neuroengineering from Brown University, Providence, RI, and the Ph.D. degree in biomedical engineering from the Johns Hopkins University School of Medicine, Baltimore, MD. He currently oversees the Applied Neuroscience programs at the Johns Hopkins University (JHU) Applied Physics Laboratory as an Assistant Program Manager, and has an appointment as an Assistant Research Professor at the JHU Whiting School of Engineerings Department of Electrical and Computer Engineering. He has worked on neuroscience technology for over a decade, focusing primarily on neuromorphic systems and closed-loop brainmachine interfaces. His research has been featured in a number of prominent scientific and engineering journals including the IEEE Transactions on Neural Systems and Rehabilitation Engineering, the IEEE Transactions on Biomedical Circuits and Systems, and the IEEE Transactions on Neural Networks.



**Carey E. Priebe** Buddha in training.